23rd ABCM International Congress of Mechanical Engineering
December 6-11, 2015, Rio de Janeiro, RJ, Brazil

NUMERICAL SIMULATION AND TRANSONIC WIND TUNNEL RESULTS FOR THE INTERSTAGE REGION OF THE SONDA III SOUNDING ROCKET FLIGHT

Eduardo Jourdan de Araújo Jorge Filho
Edson Basso
João Luiz F. Azevedo
Maria Luísa Collucci da Costa Reis
João Batista Pessoa Falcão Filho
Instituto de Aeronáutica e Espaço (IAE), Divisão de Aerodinâmica (ALA), Pça. Marechal Eduardo Gomes, 50, CEP: 12228-904, São José dos Campos, São Paulo, Brasil
eduardojourdan92@gmail.com, edsonbss@gmail.com, joaoluiz.azevedo@gmail.com, mluisareis@yahoo.com.br, jb.falcaofilho@gmail.com

Abstract. *This paper investigates the flowfield around the SONDA III sounding rocket. The first-stage of the vehicle consists of a solid-rocket motor with almost twice the diameter of the second stage. This characteristic requires the placement of a frustum to couple the two stages. Fins are attached to the same region of the vehicle to stabilize the second-stage flight, resulting in a geometrically complex configuration. This constructive characteristic creates flow disturbances around the vehicle in the transonic regime, which requires experimental and numerical investigation. For numerical simulation, complex meshes are necessary and convergence difficulties are expected. A test campaign was carried out at the Transonic Wind Tunnel (TTP) of the Institute of Aeronautics and Space (IAE) to study the aerodynamic phenomena in the inter-stage region on a half-model, scale 1:8, installed on the side wall of the test section. The model has pressure tap outputs for surface pressure imprint applied to the model. The flow conditions investigated in the experimental tests encompass Mach numbers from 0.1 to 1.1. A commercial solver is used for the Reynolds-averaged Navier-Stokes numerical simulations. This paper compares results from both numerical and experimental approaches.*

Keywords: *Transonic Flow, Computational Fluid Dynamics (CFD), Sonda III Sounding Rocket*

1. INTRODUCTION

The Aerodynamic Division (ALA) of the Institute of Aeronautics and Space (IAE) has carried out research in order to assess the flowfield over the Sonda III sounding rocket vehicle. The Sonda III was developed by the IAE as a two-stage vehicle with a 0.30 m diameter second stage, capable of carrying a payload of approximately 100 kg up to an altitude of 600 km. It is one of the sounding rocket of the Sonda family, which started with Sonda I, first launched in 1965. Sonda III was designed in 1971 and launched in 1976. Because of the complex aerodynamic phenomena presented in the inter-stage sector, its study is still important and very useful in providing knowledge for the design of new spacecrafts within the Institute.

Figure 1 (a) shows a picture of the Sonda III being launched. A first model in scale 1:20 of the complete vehicle was conceived, as shown in Fig. 1 (b), and mounted for tests in the test section of the Pilot Transonic Wind Tunnel (TTP) of IAE-ALA. The tunnel has a test section of 0.30 m x 0.25 m and a main compressor of 830 kW continuously drives it. Automatic control systems guarantee stable conditions of Mach number (from 0.2 to 1.1), stagnation pressure (from 50 kPa to 125 kPa), stagnation temperature and humidity, at the tunnel's test section. An intermittent mass injection system operating at Mach number 1.9 allows the tunnel to achieve Mach numbers up to 1.3 during at least 30 seconds (Falcão Filho and Mello, 2002).

The test campaign assessed global force coefficients and pressure distribution over the surface of the model (Falcão Filho, 2011). These tests evidenced the importance of exploring the inter-stage region of the model (highlighted by a yellow circle in Fig. 1 (b)). Due to this conclusion a new research effort was planned, which included the construction of a new model of the complete vehicle in scale 1:8, giving special attention to this region. Because of its blockage area ratio of 5% and its length, which surpassed the total length of the test section in 15%, the model was conceived as a half-model to be mounted on the side wall of the tunnel. Figure 1 (c) shows the model, with the first stage shortened to accommodate within the test section. As the main interest is on the inter-stage region, there is no significant loss in the flow behavior when adopting this idea.

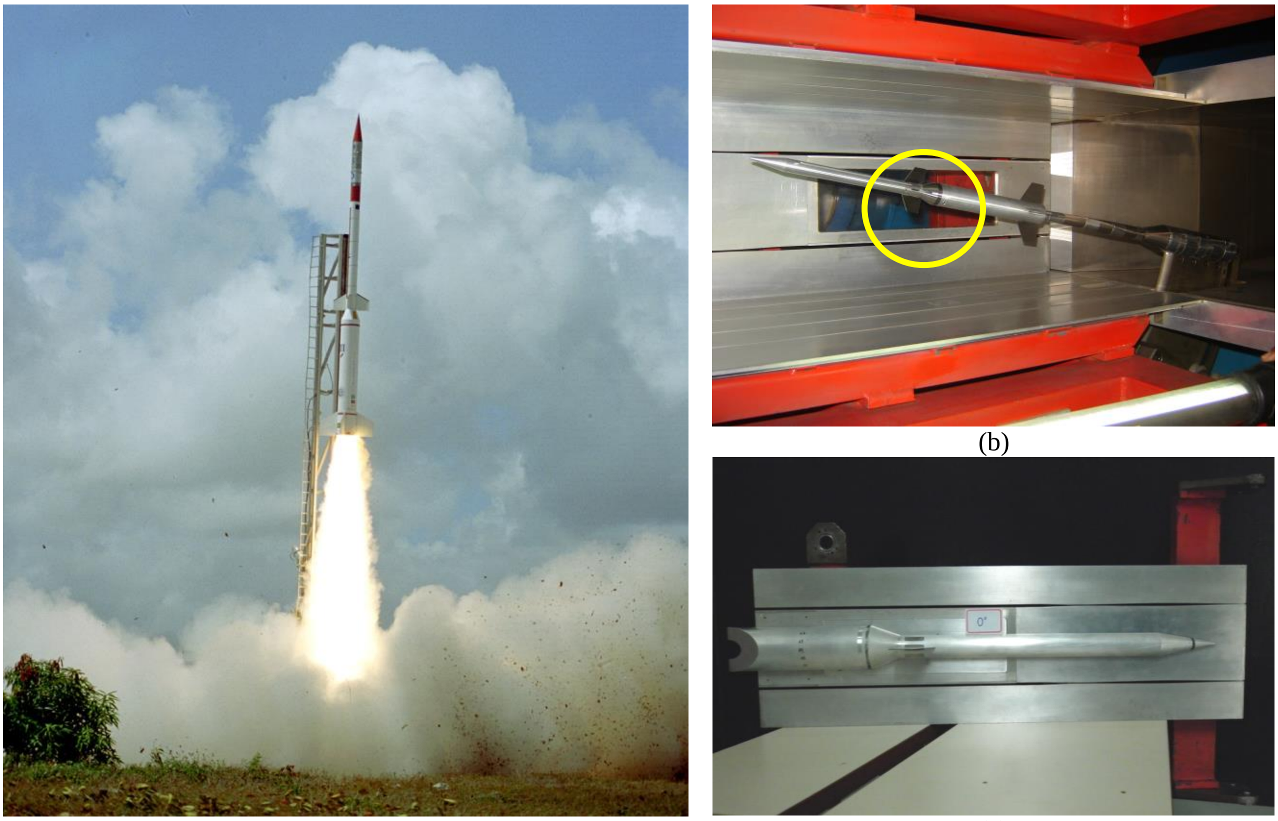

(a) (b) (c)

Figure 1. (a) Launch of Sonda III, (b) complete model in scale 1:20 installed in the test section of TTP, (c) half-model in scale 1:8 mounted in the side wall of the test section of TTP with one fin perpendicular to the wall.

To better assess the physical phenomena in flow field around the vehicle, numerical simulation was employed to complement wind tunnel information. The half-model used in this test campaign has 154 pressure taps to measure local static pressures. Some difficulties found in the tests, such as the finite number of pressure taps on the model surface, limit information about the pressure distribution on the vehicle. As Computational Fluid Dynamics (CFD) solutions are observable for the whole flow field, numerical results can complement the experimental data.

Numerical simulation has emerged as appropriate in helping the interpretation of aerodynamic physical phenomena. One can mention the leadership of Kutler (1985) in researches undertaken in NASA (National Aeronautics and Space Administration). The author developed computational codes to investigate the real flow around space vehicles. At that time, he pointed the great importance of these solutions compared with other theoretical approaches, although challenges should be overcome such as: mesh generation, turbulence model, computational capacity and solution methodology. Resende (2004) described the use of numerical simulation by EMBRAER - Empresa Brasileira de Aeronáutica, in the development of its aircrafts in an evolutionary process.

In IAE, and particularly in the Aerodynamics Division (ALA), real flows around space vehicles has been investigated since a long time ago as demonstrated by Azevedo (1988), through various research lines, being this present study one of them. In the present paper some results for Mach number 0.75 obtained with both techniques, experimental and numerical calculation, are shown. A comparison of the two methods was made for the pressure distribution on the model surface in the longitudinal direction between the fins.

The pressure coefficient is defined by (Anderson, 2007) as

$$c_p \equiv \frac{p - p_\infty}{q_\infty A}\,, \tag{1}$$

where p is the local pressure, p_∞ is the pressure at freestream condition, A is a reference area and q_∞ is the dynamic pressure at free-stream condition and defined by

$$q_\infty \equiv \frac{1}{2}\rho_\infty V_\infty^2\,, \tag{2}$$

where ρ_∞ and V_∞ is density and velocity at freestream condition.

2. THE EXPERIMENTAL CAMPAIGN

The test campaign with the half-model in several configurations was carried out at the TTP transonic wind for undisturbed Mach number condition from 0.1 to 1.1. The model was conceived for three distinct configurations: without fins in the inter-stage region, with one fin at the model centerline, and with two fins at 45^o and -45^o from the model centerline. In all situations, the half-model was positioned with a 4 mm gap from the tunnel wall. The gap avoids the development of the boundary layer from the test wall over the model surface. The gap also imitates the absence of wall, originating results as for the complete model. The Sonda III model used in the tests has 154 pressure taps located around the inter-stage part, arranged in 22 longitudinal stations, and with 7 pressure taps circumferentially distributed at each station.

Results revealed a variation of flow behavior for undisturbed Mach numbers above 0.75. The solution showed an operation near the critical point, *i.e.*, local Mach number 1.0. In this paper, results for angle of attack equal to 0^o, Mach number regime equal to 0.75, and model with one fin mounted perpendicularly to the tunnel wall, are presented. Figure 1c shows details of this installation.

3. THE NUMERICAL CODE

The numerical code used to simulate the airflow was the CFD++®. The simulation was based on the Reynolds-Averaged Navier-Stokes equations, RANS, in a three dimensional formulation. The Spalart-Allmaras one equation [5] turbulence model was chosen in these simulations. The discretization scheme is based on finite volumes in an unstructured mesh. An implicit method of time marching associated with a multi-grid scheme was adopted. The complete Sonda III model was simulated in free-flight conditions, *i.e.*, the walls of the TTP test section were not considered. This can be done because the TTP test section walls are slotted, just for purpose to achieve results without wall influence. The computational mesh has a symmetrical plane crossing the centerline of the model, which coincides with the longitudinal base of the half model. The second stage fin of the vehicle is perpendicular to the symmetry plane.

The distance of the farfield boundary is about 37 diameters of the first stage of the model. Mesh volumes were clustered near the surface of the model in order to capture the boundary layer developed on the body. Figure 2(a) shows the mesh, with focus on inter-stage and fin region, and Fig. 2(b) shows a detail of the leading edge mesh. Stretching of 16% rate near the fuselage and the fin was adopted to save the number of calculation points and satisfy the y+ condition for a value of 1, as required by the Spalart-Allmaras turbulence model. This resulted in 50 points within the boundary layer region. The history of maximum residue was monitored and the solution was considered converged after a decrease of four orders of magnitude. The simulation was undertaken in a parallel environment using 24 processors in a cluster of computers. The total convergence time for the solution was 15 hours.

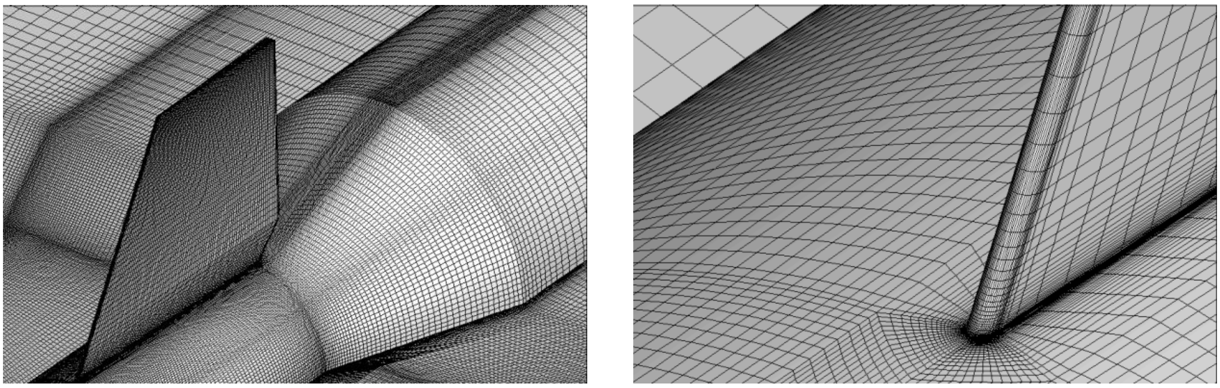

(a) (b)

Figure 2. The Sonda III mesh. a) Inter-stage region. b) Detail of the leading edge of the fin.

4. RESULTS

Some results are presented in cut planes along grid axis coordinate, as shown in Fig. 3. The planes indicated by A5, A6 and A7 are placed in 22.5, 45 and 67.5 degrees from the plane A4, which pass through the fin, perpendicular to symmetry plane. Figure 4(a) shows a three-dimensional view with Mach number distribution over the symmetrical plane, for freestream Mach number 0.75 in a view close to the model. Observe the decelerating regions at the model's tip and approaching the frustum. On the other hand, one can see two expansion regions just after the first cone and just after the frustum. Figure 4(b) shows the pressure contours over the symmetrical plane and surface model of the vehicle. From this figure, one can observe a more detailed view of the expansion waves after the first cone and the inter-stage frustum, with a severe drop in the pressure levels at the second one. These results are in agreement with the theory, and a very small region of supersonic flow after the expansion corner of the frustum was captured by the code.

The disturbances caused by the fin are very small, as can be seen on Fig. 5(c) to (e). In these sequences is possible to see how the disturbances on the wake of the fin are smeared rapidly by the code. A cause for this is the mesh, which are not very refined in this region. Another reason is due to the class in wich the code was developed (RANS) which is known for damping vortices on wakes very fast. Figures 5(d) e 5(e) show the existence of a small variation in properties along the circumferential direction. To better understand these variations were made a sequence of figures shown in Figure 6. With these figures, it is noticed that the planes A5, A6 and A7 shown in Fig. 6 (b), (c) and (d), respectively, have Mach numbers contours substantially the same. An interesting feature is noticed when comparing Figs. 6(a) with 6(b), or 6(c), or even Fig. 6(d). Through these comparisons it is possible to note how the wake of the fin virtually eliminates the supersonic flow region after the corner of the frustum. Although this region is small, it can produce a shock, which can detach the boundary layer, causing an asymmetry in the flow, which may be important for an aeroelastic analysis of the vehicle.

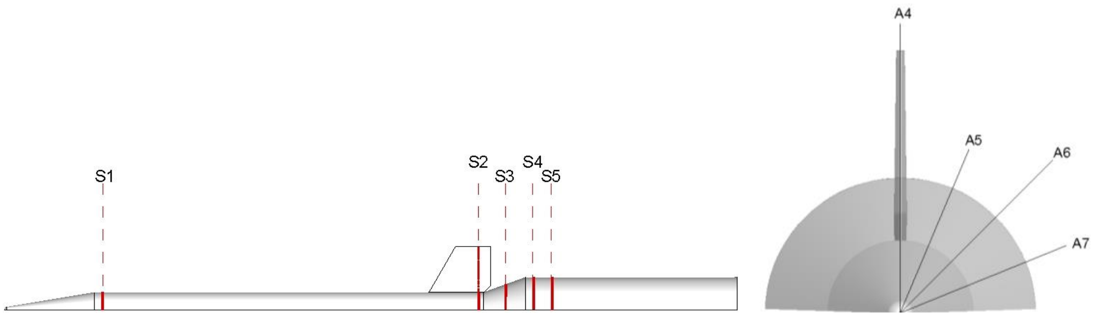

(a) (b)

Figure 3. (a) Cut planes positions perpendicular to longitudinal direction; (b) Cut planes positions parallel to longitudinal direction.

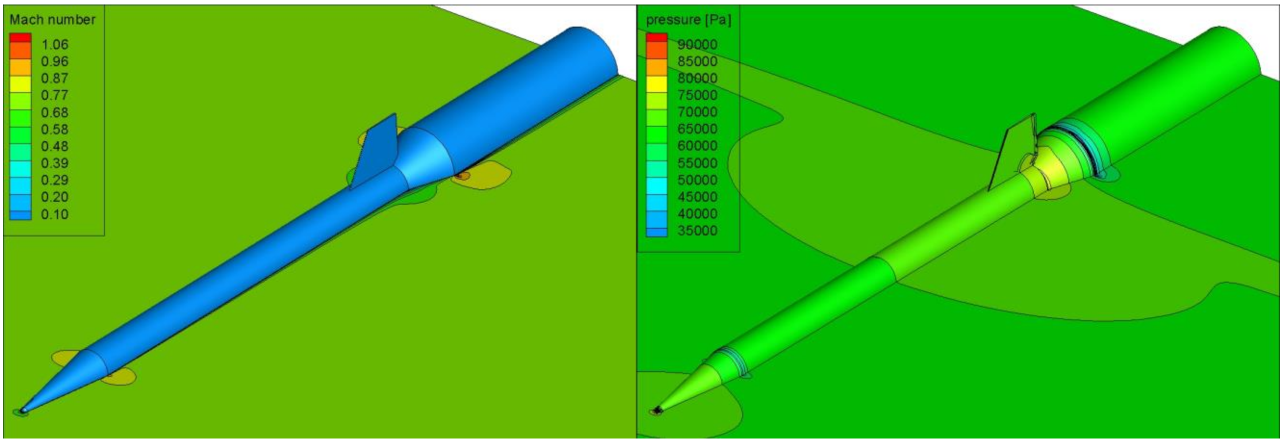

(a) (b)

Figure 4. (a) Mach number contours on symmetrical plane and (b) static pressure contours on the surface of the Sonda III rocket.

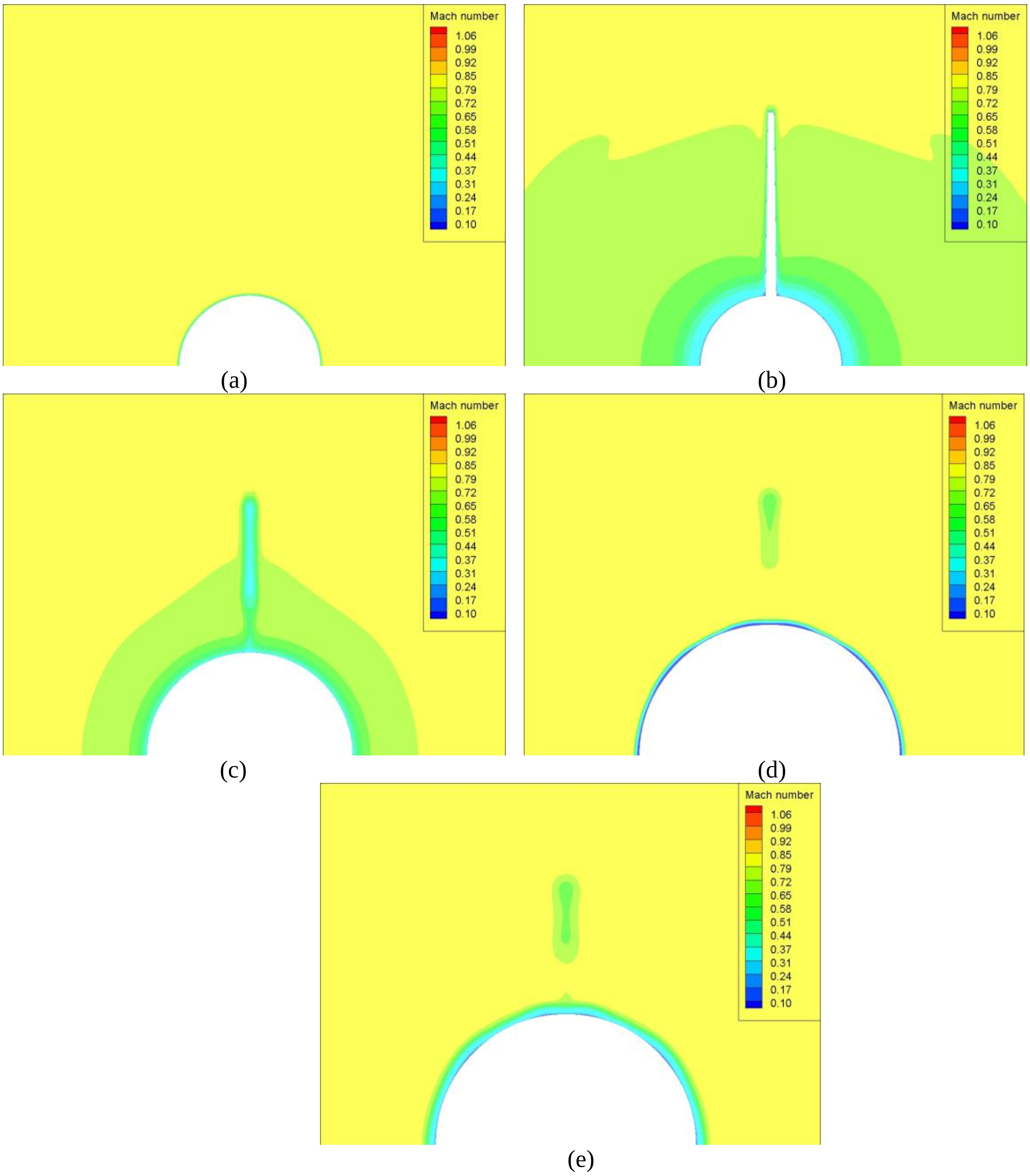

Figure 5. Mach number contours on planes along the longitudinal direction of the vehicle: (a) plane S1, (b) plane S2, (c) plane S3, (d) plane S4 and (e) plane S5, indicated in Fig. 3.

Figure 7 shows the Cp distribution along each intersection line between the surface and the planes named A4, A5, A6 and A7 in Fig. 3. In Fig. 7, it is possible to see that numerical results are in a good agreement with experimental data from the nose area to near the fin leading edge, and downstream of the frustum. Only the region around the fin shows some differences in the results. Figure 8 is a detailed view of Fig. 7 showing that, except for the result in plane A4, which pass through the fin, the values of Cp are very close among each other. One can observe that in x=0.535 the curve for A5 plane is more influenced that A6 results. In fact, both A6 and A7 results are practically identical, as expected. The points representing results for A4 plane has a gap, due to the lack of values for the surface on the top of the fin.

The comparison between computational and experimental results is shown on Fig. 9. Both simulation and experimental data are taken on the surface intersection with plane A6, plotted only around the frustum. A good agreement was obtained in front of the cone, moving away from experimental data as it approach the leading edge. After the corner the pressure is recovered a little bit slower than in the wind tunnel. A possible cause may be the recirculating flow at this point, as showed by Fig. 10. It is not possible to say that such a feature of the flow is present on wind tunnel results because we have a few pressure taps on this region. The authors are considering to use another visualization technique such as laser velocimetry to investigate the behavior of boundary layer along frustum and downstream of it.

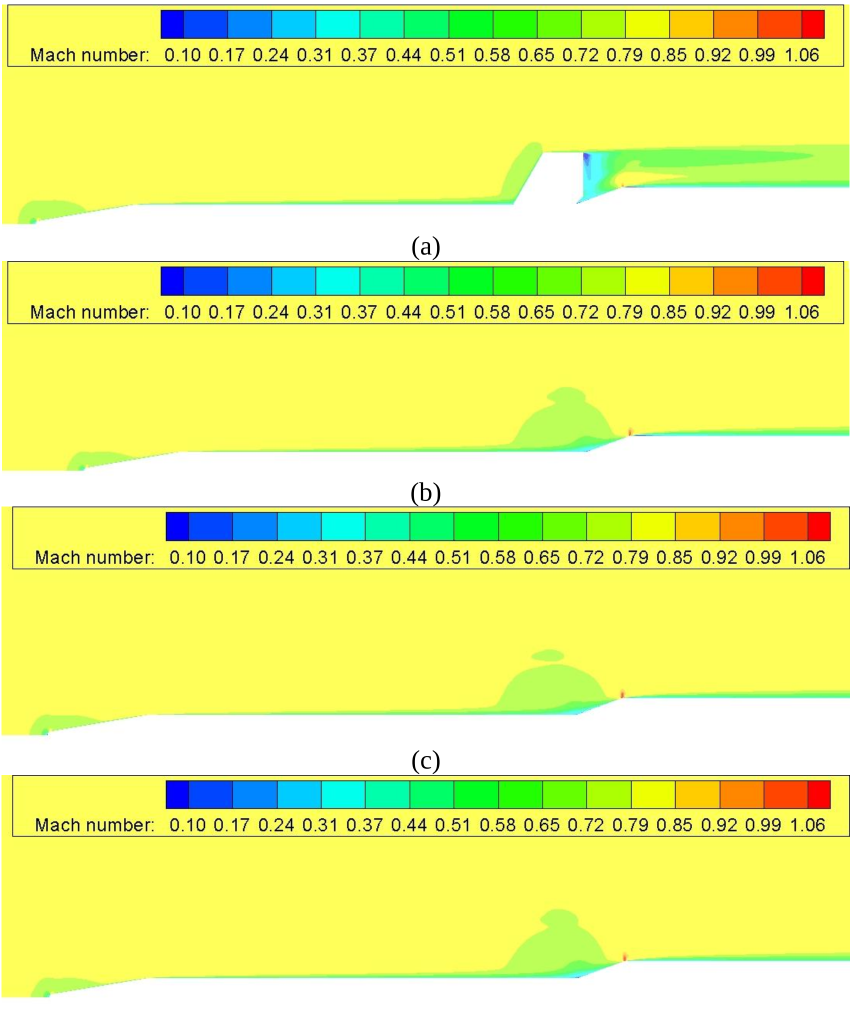

Figure 6. Mach number contours: (a) plane A4, (b) plane A5, (c) plane A6 and (d) plane A7, as indicated in Fig. 3.

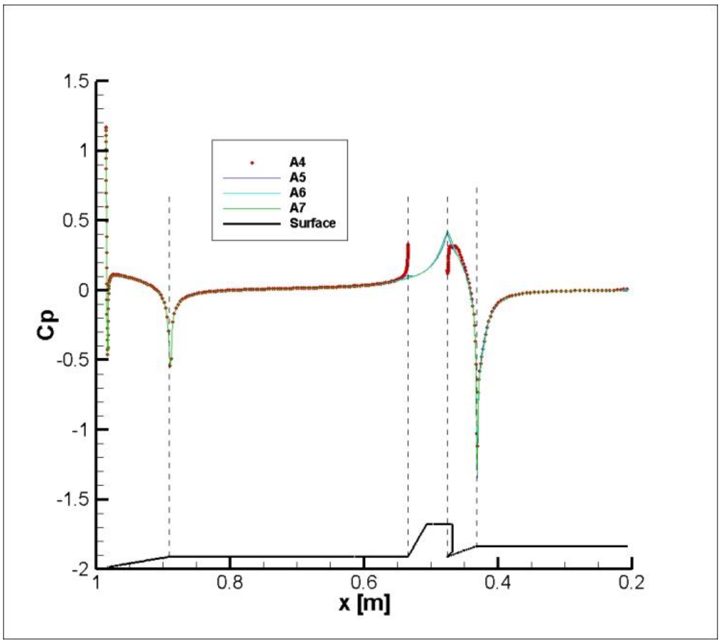

Figure 7. Cp distribution over the surface, along surface intersection lines with planes A4, A5, A6 and A7, as indicated in Fig. 3.

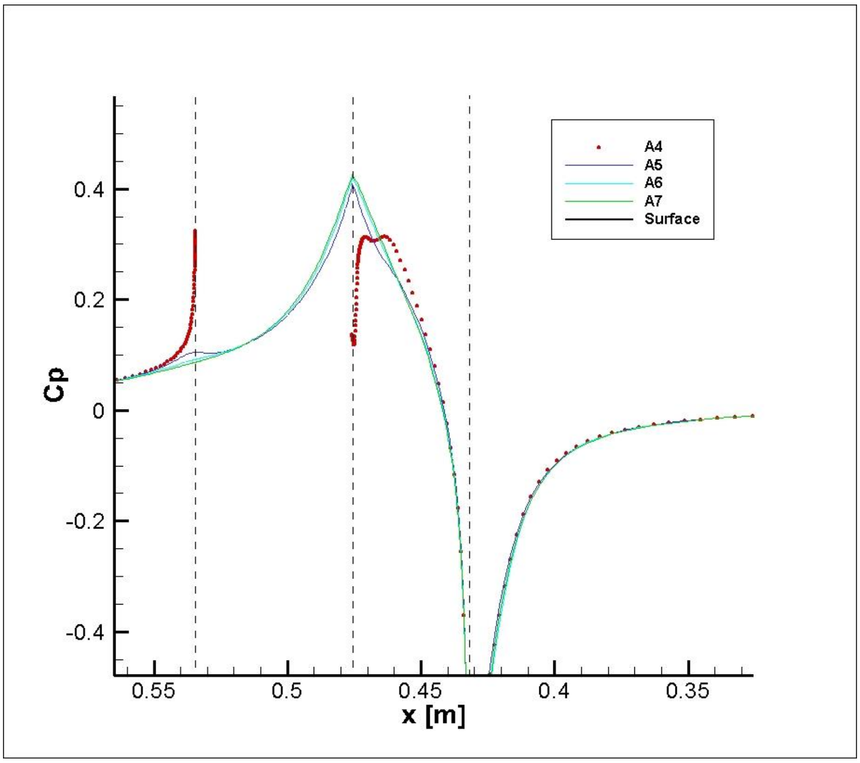

Figure 8. A detailed view of Fig. 7, near the fin abscissa.

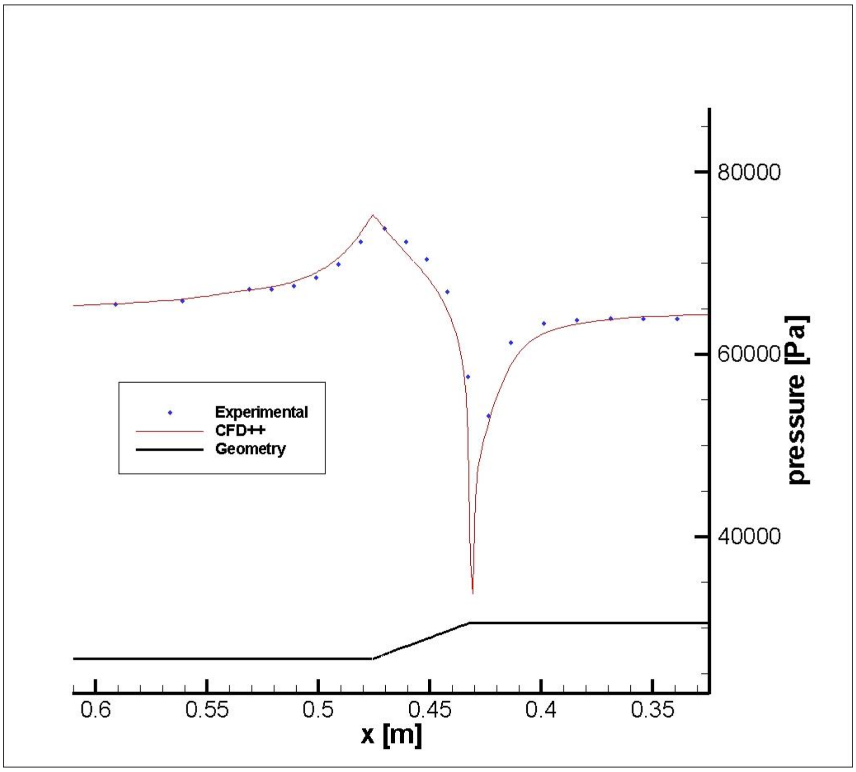

Figure 9. Comparison between numerical results and experimental data, for surface intersection with plane A6 line.

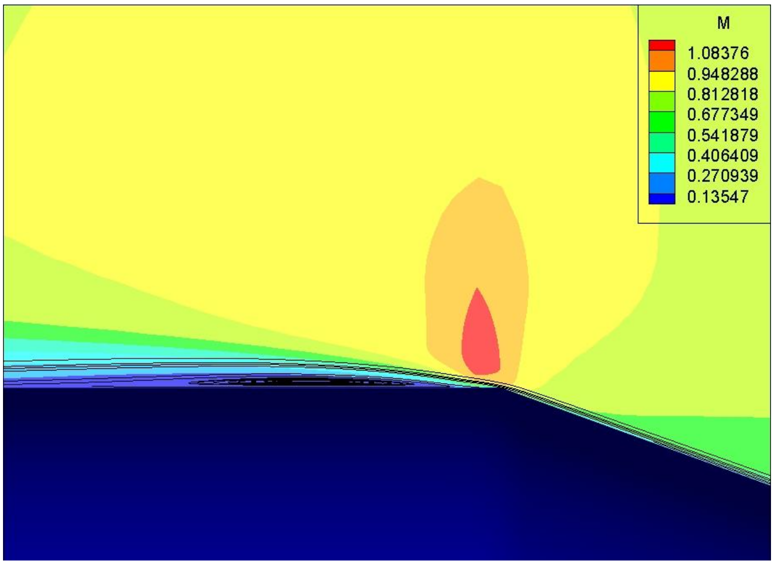

Figure 10. A windowed view near the frustum with streamlines showing a recirculating zone.

5. CONCLUDING REMARKS

In this paper, we analyzed the flowfield around Sonda III sounding rocket, with one fin. Both experimental and simulation was carried out to investigate some features of the flow near inter-stage cone frustum and fin. The model represents half vehicle, mounted in a plate near one slotted wall of the tunnel. Due to the presence of slots and flow conditions at entrance, it is possible to achieve results without wall´s disturbances. Numerical simulations was conducted imposing symmetry boundary condition to account the effect of such tunnel particularity. The results shows that both results are in a good agreement, in most part of the flow over the surface. The influence of the fin is very small, restricted on the wake and regions near both sides of the fin. The Mach number of the flight condition analyzed in conjunction of some aspects of the geometry shows a small region of supersonic flow. This small region is not sufficient to produce strong shocks and rarefaction waves, but a detached flow was observed at the corner of frustum. Others visualization techniques are under consideration to try understand some particularities of the problem.

6. ACKNOWLEDGEMENTS

The authors gratefully acknowledge the partial support for this research provided by Conselho Nacional de Desenvolvimento Científico e Tecnológico, CNPq, under the Research Grants No. 560200/2010-2, No. 309985/2013-7, No. 400844/2014-1, No. 443839/2014-0, No. 185258/2014-0, No. 574004/2008-4, and No. 280183/2015-3. The authors are also indebted to the partial financial support received from Fundação de Amparo à Pesquisa do Estado de São Paulo, FAPESP, under the Research Grants No. 2013/07375-0 and No. 2008/57866-1.

7. REFERENCES

Anderson, J.D.Jr., 2007, “Fundamentals of Aerodynamics”, 4th edition, McGraw-Hill International Edition.

Azevedo, J.L.F., 1988, “Transonic Aeroelastic Analysis of Launch Vehicle Configurations,” Ph.D. Thesis, Stanford University, California, USA, 155 p.

Falcão Filho, J.B.P., Mello, O.A.F., 2002, “Descrição Técnica do Túnel Transônico Piloto do Centro Técnico Aeroespacial,” Proceedings of the 9th Brazilian Congress of Thermal Engineering and Sciences, Caxambu, MG.

Falcão Filho, J.B.P., Reis, M.L.C.C., Morgenstern, A.Jr., 2011, “Experimental Results from the Sounding Vehicle Sonda III Test Campaign in the Pilot Transonic Wind Tunnel,” Journal of Aerospace and Technology and Management, Vol.3, No.3, pp. 311-324 (DOI: 10.5028/jatm.2011.03033111).

Kutler, P., 1985, “A Perspective of Theoretical and Applied Computational Fluid Dynamics,” AIAA Journal, Vol. 23, No. 3, pp. 328-341.

Resende, O.C., 2004, “The Evolution of the Aerodynamic Design Tools and Transport Aircraft Wings at Embraer,” Jornal of the Brazilian Society of Mechanical Sciences and Engineering, Vol. XXVI, No. 4, pp. 379-390.

Wilcox, D.C., 2006, “Turbulence Modeling for CFD”, 3rd ed., DCW Industries, Inc., La Canada, CA.

8. RESPONSIBILITY NOTICE

The authors are the only responsible for the printed material included in this paper.